Int. J. Heat Mass Transfer. Vol. 28, No. 11, pp. 2049–2060, 1985
Printed in Great Britain

0017–9310/85 $3.00 + 0.00

Two-dimensional heat transfer and critical radius results for natural convection about an insulated horizontal cylinder

E. M. SPARROW and S. S. KANG
Department of Mechanical Engineering, University of Minnesota, Minneapolis, MN 55455, U.S.A.

(*Received* 25 *February* 1985 *and in final form* 7 *May* 1985)

Abstract—The two-dimensional (i.e. radial and circumferential) heat transfer and fluid flow problem for a fluid-carrying, insulated horizontal cylinder which loses heat to air by natural convection was analyzed by solving the differential form of the conservation laws. The resulting conjugate problem encompassed conduction in the insulation layer and natural convection in the ambient air. A one-dimensional, radial heat flow model of the problem was also investigated in detail, and the circumferential-average natural convection heat transfer coefficients needed for its evaluation were respectively taken from the commonly used correlations of McAdams, Morgan, and Churchill and Chu. It was found that the correlation-related spread of the heat transfer results from the one-dimensional model was greater than the differences between the one- and two-dimensional results. The use of the Morgan correlation gave the most accurate set of one-dimensional heat transfer results (i.e. best agreement with the two-dimensional results). For the critical radius, the standard $h_o r^*/k_{ins} = 1$ criterion led to significant errors and should no longer be used. The critical radius results from the one-dimensional model, although correlation-dependent and deviant from the two-dimensional results, can be calculated efficiently and accurately from the criterion $h_o r^*/k_{ins} = 3n/(1+n)$, where n is an exponent which can be determined for each specific Nusselt–Rayleigh correlation.

INTRODUCTION

THE RECENT years have witnessed heightened interest in the innovative use of insulation to conserve thermal energy. Notwithstanding this, the venerable critical radius concept continues to be routinely used in sizing the insulation thickness for pipes, despite the fact that certain underlying assumptions have never been definitively evaluated. The issue of specific concern here is the neglect of circumferential variations in the analysis which is used in the determination of the critical radius. If the pipe is in crossflow, either in forced convection or in natural convection, circumferential variations of the external heat transfer coefficient are a reality of nature. These variations in the transfer coefficient induce circumferential components in the heat conducted through the insulation, thereby invalidating the assumed radial conduction that is the cornerstone of the standard critical radius analysis.

In this paper, an analysis is made of an insulated horizontal cylinder which loses heat to air by natural convection, with full account being taken of circumferential variations of the convective heat transfer coefficient and of circumferential conduction in the insulation. There are two reasons for focusing here on the natural convection problem rather than on the forced convection problem. First, owing to the relatively high heat transfer coefficients for forced convection, the external convective resistance is small relative to the conductive resistance in the insulation. As a result, the critical radius is irrelevant for the conditions most commonly encountered in forced convection crossflows (i.e. the critical radius is smaller than the outer radius of the uninsulated pipe). On the other hand, the critical radius concept is applicable to a broad range of operating conditions for natural convection about an insulated horizontal cylinder. Second, the natural convection problem is more complex and more challenging because the fluid flow about the cylinder is affected by the circumferential variations of the surface temperature of the insulation, which is not so in the forced convection case.

In the problem to be investigated here, the circumferential variation of the external heat transfer coefficient depends on the circumferential variation of the surface temperature, and the converse is equally true. The surface temperature can be obtained by solving the heat conduction problem in the insulation for a given external heat transfer coefficient, while the heat transfer coefficient comes from solving the natural convection problem for a given surface temperature. Both the surface temperature and the convective heat transfer coefficient are unknown and can be found only by solving the *conjugate* conduction–convection problem encompassing the insulation and the fluid exterior to the cylinder. Both the conduction and the natural convection problems which make up the aforementioned conjugate problem are solved here from first principles, that is, by solving the differential equations which represent the conservation laws for energy, mass and momentum.

The solutions obtained here are governed by five parameters: (1) the Rayleigh number characterizing the external natural convection, (2) the ratio of the thermal conductivities of the insulation and the fluid external to the cylinder, (3) the ratio of the outer and inner

NOMENCLATURE

C coefficient in Nu_o, Ra_o power law
d_i inner diameter of insulation and outer diameter of pipe
d_{ii} diameter of pipe bore
d_o outer diameter of insulation
g acceleration of gravity
h_i pipe-flow heat transfer coefficient
h_o natural convection heat transfer coefficient
k_{air} thermal conductivity of air
k_{ins} thermal conductivity of insulation
Nu_i pipe-flow Nusselt number
Nu_o circumferential-average natural convection Nusselt number
n exponent in Nu_o, Ra_o power law
Pr Prandtl number
Q heat transfer rate per unit length
R thermal resistance, equation (18)
Ra Rayleigh number, $[g\beta(T_b - T_\infty)d_i^3/\nu^2]Pr$
Ra_o Rayleigh number, $(d_o/d_i)^3\phi_o Ra$
Ra' Rayleigh number, $(d_o/d_i)^3 Ra$
r radial coordinate
r_i inner radius of insulation and outer radius of pipe
r_o outer radius of insulation
r^* critical radius
T temperature
T_b fluid bulk temperature in pipe bore
T_i temperature at d_i and d_{ii}
T_o temperature at d_o
T_∞ ambient temperature
U, V dimensionless velocities, equation (2)
u, v radial and circumferential velocities.

Greek symbols

α thermal diffusivity
β coefficient of thermal expansion
η dimensionless radial coordinate, r/d_o
η_{max} outer boundary of convective solution domain
θ circumferential coordinate
ν kinematic viscosity
ϕ dimensionless temperature, $(T - T_\infty)/(T_b - T_\infty)$
Ψ dimensionless streamfunction
Ω dimensionless vorticity.

Subscript

crit critical condition, corresponding to Q_{max}.

diameters of the insulation, (4) the Nusselt number characterizing the heat transfer at the bore of the cylinder, and (5) the Prandtl number of the external fluid. Aside from the Prandtl number, which was fixed at 0.7 (air), all of the other parameters were varied during the course of the numerical solution of the problem.

The presentation of results will be subdivided into three parts. In the first part, dimensionless heat transfer rates obtained from the solutions of the aforementioned conjugate problem are compared with corresponding results from the conventional one-dimensional radial heat flow model. In implementing the one-dimensional model, the needed values of the circumferential-average natural convection heat transfer coefficient were obtained from the three most-used correlations in the literature [1–3]. The comparisons were made not only to show the differences between the results from the different models, but also to examine whether the degree of accuracy of the critical radius predictions is (or is not) correlated with the accuracy of the heat transfer predictions. Another feature of the comparisons is the demonstration of the sensitivity of the one-dimensional results to the various correlations employed for the circumferential-average heat transfer coefficient.

The second part of the presentation of results conveys values of the critical radius from both the two-dimensional conjugate model and the one-dimensional model. For the latter, two approaches were used in the determination of the critical radius. One approach is the standard textbook criterion $h_o r^*/k_{ins} = 1$, where r^* is the critical radius, h_o is the circumferential-average heat transfer coefficient at the outer surface of the insulation, and k_{ins} is the thermal conductivity of the insulation. This criterion is approximate because it is derived by neglecting the dependence of h_o on the outer radius and on the surface-to-ambient temperature difference. The other approach determines the exact value of r^* consistent with the one-dimensional model. Further, for the one-dimensional model, values of the critical radius are obtained and presented for each of the aforementioned three correlations of h_o.

The presentation of results concludes with a set of representative circumferential temperature distributions at the outer surface of the insulation, as obtained from the two-dimensional conjugate model.

A survey of the literature affirmed that heat transfer from an insulated horizontal cylinder by natural convection has, in the past, been treated only as a radially one-dimensional process, without regard for circumferential variations. The classical critical radius criterion $h_o r^*/k_{ins} = 1$ was upgraded in [4] to account for the dependence of h_o on the outer radius and on the surface-to-ambient temperature difference for situations where the circumferential-average Nusselt

number varies as a power of the Rayleigh number. In [5], a more complex Nusselt–Rayleigh relation (i.e. not a power law) was considered, yielding a correspondingly complex representation for the critical radius. In this regard, it will be demonstrated later that the method of [4] can also be applied to Nu, Ra relations which are not power laws. Other recent modifications of the critical radius have taken account of radiative transfer [6] and of surface heat generation [7].

ANALYSIS

The physical situation to be analyzed is pictured schematically in Fig. 1. Depicted there is an annular layer of insulation (inner and outer radii r_i and r_o, respectively, thermal conductivity k_{ins}) which covers a horizontal cylinder whose outer radius is also equal to r_i. The cylinder is a circular pipe which contains a flowing fluid whose bulk temperature at a representative axial station is T_b. The insulated cylinder is situated in an air environment whose temperature T_∞ is less than T_b. Aside from the natural convection motions induced by the presence of the cylinder, the air is quiescent.

The temperatures T_i and T_o at the inner and outer surfaces of the insulation will find their own levels and circumferential distributions consistent with the participating heat transfer processes. In particular, if, as expected, the heat transfer coefficient at the outer surface decreases with increasing values of the circumferential coordinate θ, the temperature should increase with θ. It is by this mechanism that the problem becomes two-dimensional.

Governing equations

To analyze the problem, the conservation laws which pertain to the insulation layer and to the fluid environment external to the insulation have to be written. In this regard, dimensionless variables are introduced as follows

$$\phi = (T-T_\infty)/(T_b-T_\infty), \quad \eta = r/d_o \tag{1}$$

$$U = ud_o/\alpha, \quad V = vd_o/\alpha, \quad \Psi = \psi/\alpha. \tag{2}$$

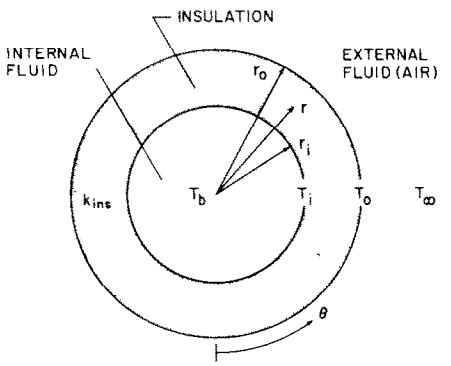

FIG. 1. Schematic representation of the physical situation to be analyzed.

For the insulation layer, the heat conduction problem is governed by Laplace's equation

$$\nabla^2\phi = 0 \tag{3}$$

where ∇^2 is the conventional Laplace operator in (η, θ) polar coordinates.

For the external fluid environment, the streamfunction/vorticity form of the conservation equations will be adopted in order to employ the numerical solution scheme that had been used effectively in [8] for the isothermal horizontal cylinder. The continuity equation is satisfied by a streamfunction defined as

$$\eta U = \partial\Psi/\partial\theta, \quad V = -\partial\Psi/\partial\eta \tag{4}$$

and it follows from the definition of the vorticity that

$$\Omega_z \equiv \Omega = -\nabla^2\Psi. \tag{5}$$

Next, the η and θ momentum equations, with respective buoyancy terms $-g\beta(T-T_\infty)\cos\theta$ and $g\beta(T-T_\infty)\sin\theta$, are merged into a single equation by cross differentiation and subsequent subtraction

$$[U(\partial\Omega/\partial\eta)+(V/\eta)(\partial\Omega/\partial\theta)]/Pr$$

$$= \nabla^2\Omega + Ra'[(\partial\phi/\partial\eta)\sin\theta + (1/\eta)(\partial\phi/\partial\theta)\cos\theta]. \tag{6}$$

The bracketed terms on the RHS represent the buoyancy, and

$$Ra' = [g\beta(T_b-T_\infty)d_o^3/\nu^2]\,Pr. \tag{7}$$

Note that Ra' is based on the known overall temperature difference (T_b-T_∞) rather than on the surface-to-ambient temperature difference $[T_o(\theta)-T_\infty]$, which is both unknown and nonuniform. The factor $1/Pr$ which multiplies the inertia terms on the LHS of equation (6) reflects the presence of α in the definition of the dimensionless velocities.

The last of the governing equations for the fluid, energy conservation, is written in the conventional form

$$U(\partial\phi/\partial\eta)+(V/\eta)(\partial\phi/\partial\theta) = \nabla^2\phi \tag{8}$$

where the absence of Pr is, again, a consequence of the definition of the dimensionless velocities.

Boundary and coupling conditions

Owing to symmetry, the problem need be solved only for the range $0 \leqslant \theta \leqslant 180°$. Furthermore, on the lines $\theta = 0$ and 180°, the conventional symmetry boundary conditions apply, i.e. $V = \partial U/\partial\theta = \partial\phi/\partial\theta = 0$, from which it follows that $\Psi = 0$ and $\Omega = 0$. The computational domain for the external fluid environment was bounded at its outer edge by a circle $\eta = \eta_{max}$ on which $T = T_\infty$ and $\phi = 0$. During the course of the work, the size of η_{max} was varied to ensure that it was large enough not to affect the heat transfer results. The velocity boundary conditions at $\eta = \eta_{max}$ and at $\eta = \frac{1}{2}$ (the outer surface of the insulation) are set forth in [8] and need not be repeated here.

The specification of the temperature conditions at

the surface of the insulation will be tailored to complement the iterative procedure to be used for solving the governing equations. A key output of each cycle of the iteration is the surface temperature distribution $\phi_o(\theta)$. To initiate the next cycle, the $\phi_o(\theta)$ distribution is used as the thermal boundary condition for the natural convection problem, thereby completing the specification of that problem. The solution of the natural convection problem yields the local heat transfer coefficient $h_o(\theta)$

$$h_o d_o/k_{air} = [-(\partial\phi/\partial\eta)_{\eta=1/2}]_{nc}/\phi_o \quad (9)$$

where the additional subscript nc is appended to indicate that the derivative is from the natural convection solution. Note also that the thermal conductivity of the convecting fluid has been designated as k_{air}, since the focus is on air.

The continuity of heat flow at the exposed surface of the insulation, in conjunction with the $h_o(\theta)$ distribution from equation (9), provides the outer boundary condition for the conduction problem. Since $-k_{ins}(\partial T/\partial r)_{ins} = h_o(T_o - T_\infty)$ for continuity, it follows that

$$[-(\partial\phi/\partial\eta)_{\eta=1/2}]_{ins} = [(h_o d_o/k_{air})(k_{air}/k_{ins})]\phi_o \quad (10)$$

in which the subscript ins on the LHS identifies the derivative as belonging to the insulation side of $\eta = \frac{1}{2}$. Since the bracketed quantity on the right is a known function of θ at this point in the iteration process, equation (10) constitutes a fully specified boundary condition for the insulation layer (note that ϕ_o is now regarded as an unknown function of θ).

The only other boundary condition which remains to be discussed is that at the inner boundary of the insulation, $r = r_i$ and $\eta = \eta_i = r_i/d_o$. It will be assumed that there is perfect thermal contact between the insulation and the outside surface of the pipe and that the pipe wall is sufficiently conducting so that its temperature is uniform both radially and circumferentially. With these assumptions, the temperature T_i at the inner boundary of the insulation is uniform and equal to the temperature of the pipe wall. When the heat transfer coefficient h_i at the pipe bore is relatively large, T_i is essentially equal to the bulk temperature T_b of the fluid flowing in the pipe, and $\phi_i = 1$. At small and intermediate values of h_i, the value of T_i is unknown and was determined as part of the aforementioned iterative solution scheme, as will now be described.

As an output from each cycle of the iteration, the derivative $\partial\phi/\partial\eta$ at $\eta = \eta_i$ was evaluated as a function of θ and then averaged over the range $0 \leqslant \theta \leqslant 180°$, and χ is used to denote the average. Then, an energy balance at the pipe wall yields

$$h_i \pi d_{ii}(T_b - T_i) = -k_{ins}\pi d_i \chi(T_b - T_\infty)/d_o \quad (11)$$

in which d_{ii} denotes the diameter of the tube bore. After introduction of ϕ from equation (1), rearrangement of equation (11) leads to

$$\phi_i = 1 + \chi/[Nu_i(d_o/d_i)(k_i/k_{ins})] \quad (12)$$

where

$$Nu_i = h_i d_{ii}/k_i \quad (13)$$

denotes the Nusselt number for the pipe flow, and k_i is the thermal conductivity of the fluid in the pipe.

With the χ value from the preceding cycle of the iteration as input, equation (12) yields the ϕ_i value to be used as the boundary condition at $\eta = \eta_i$ (inner boundary of insulation) for the next cycle. However, when Nu_i is sufficiently large, this process can be bypassed, since, for that case, the boundary condition $\phi_i = 1$ can be used for all cycles of the iteration.

Numerical solutions

The solution of the governing differential equations and boundary conditions was accomplished by finite differences. For the natural convection portion of the problem, the discretization of the differential equations and the numerical scheme are both amply described in [8]. As already noted, the external boundary $\eta = \eta_{max}$ of the solution domain was varied to ensure the accuracy of the results, with larger values of η_{max} required for smaller values of the Rayleigh number. Overall, η_{max} ranged between 5.5 and 40. The finite-difference grid for the natural convection domain consisted of 25×28 points (circumferential $\times$ radial), with more dense deployment of the points adjacent to the surface of the insulation and in the plume.

The finite-difference grid for the conduction problem in the insulation was made up of 25×25 points, the circumferential distribution of which matched that for the natural convection domain. Radially, the grid was made somewhat finer adjacent to the inner and outer boundaries than in the remainder of the conduction domain.

For a given case defined by fixed values of the parameters, the numerical solution was initiated by making use of the results from a preceding, related case. In particular, the $\phi_o(\theta)$ distribution for the preceding case was used as the boundary condition for the natural convection problem, which was solved to give the distribution of $h_o d_o/k_{air}$ with θ. This distribution was, in turn, used in conjunction with equation (10) to provide the $\eta = \frac{1}{2}$ boundary condition for the conduction problem in the insulation layer. The $\eta = \eta_i$ boundary condition for the conduction problem was provided by equation (12), with χ from the solution of the preceding case.

The solution of the conduction problem yielded the $\phi_o(\theta)$ distribution needed to initiate the solution of the natural convection problem for the next cycle of the iteration, and the process was continued in this way until convergence was achieved. Typically, 70–100 cycles were required for convergence. It should be noted that both the natural convection and heat conduction solutions which comprise each cycle of the iteration are, in themselves, iterative.

Parameters

During the analysis presented in the preceding parts of the paper, several parameters were encountered. The

parameters will now be brought together and their numerical values assigned. The choice of the Rayleigh number definition is made to complement the presentation of results, where the effect of changing the insulation thickness is investigated for a given physical situation characterized by a pipe of outer diameter d_i and overall temperature difference $(T_b - T_\infty)$. Correspondingly,

$$Ra = [g\beta(T_b - T_\infty)d_i^3/\nu^2]\,Pr \tag{14}$$

The overall range of Ra investigated here extended from 10 to 10^5. The Prandtl number for the natural convection problem was fixed at 0.7.

The other parameters which were varied during the course of the investigation include

$$k_{ins}/k_{air}, \quad d_o/d_i, \quad \text{and} \quad Nu_i. \tag{15}$$

The k_{ins}/k_{air} ratio was assigned values of 2, 3, 4 and 5. Smaller values were also considered; for example, $k_{ins}/k_{air} = 1.5$, but for that case it was found that $Ra < 10$ in order that the critical radius exist (i.e. that $r^* > r_i$). Since $Ra < 10$ is unrealistically small for heated horizontal cylinders, results for cases with $k_{ins}/k_{air} < 2$ will not be presented.

The diameter ratio d_o/d_i was varied over the range from 1 to 6. Note also that the Rayleigh number Ra' which appears as the coefficient of the buoyancy term in equation (6) is related to the Rayleigh number Ra [equation (14)] used to parameterize the solutions via

$$Ra' = (d_o/d_i)^3 Ra. \tag{16}$$

For the pipe-flow Nusselt number Nu_i, two extreme values were employed, namely, $Nu_i = \infty$ and $Nu_i = 4$. The latter corresponds to fully-developed laminar pipe flow and is, approximately, the mean of the values for uniform wall temperature and uniform wall heat flux. With the view of attaining the lowest realistic value of the pipe-flow heat transfer coefficient h_i, the choice of $Nu_i = 4$ was supplemented by taking the thermal conductivity k_i of the fluid in the pipe as k_{air}. Therefore, the ratio k_i/k_{ins} which appears in equation (12) was evaluated as k_{air}/k_{ins} for the $Nu_i = 4$ case.

One-dimensional model

The rate of heat transfer Q per unit length from the insulated cylinder to the ambient air is given by the one-dimensional radial heat flow model as

$$Q/k_{ins}(T_b - T_\infty) = 2\pi/R \tag{17}$$

where

$$R = 2(k_{ins}/k_{air})(1/Nu_i + 1/Nu_o) + \ln(d_o/d_i). \tag{18}$$

The pipe-flow Nusselt number Nu_i has already been defined by equation (13), and Nu_o, the circumferential-average Nusselt number for the external natural convection, is

$$Nu_o = h_o d_o/k_{air} \tag{19}$$

in which h_o is the circumferential-average heat transfer coefficient.

In evaluating the one-dimensional model, values of Nu_o were obtained from each of the three most widely accepted correlations for natural convection about an isothermal horizontal cylinder. The correlations of McAdams [1] and Morgan [2] are expressed by power-law segments of the form

$$Nu_o = CRa_o^n \tag{20}$$

while that of Churchill and Chu [3] is

$$Nu_o = C_1 + C_2 Ra_o^{1/4} \tag{21}$$

in which C_2 depends on the Prandtl number and was evaluated here at $Pr = 0.7$. The Rayleigh number Ra_o and its relationship to the Rayleigh number Ra of the foregoing analysis are

$$Ra_o = [g\beta(T_o - T_\infty)d_o^3/\nu^2]Pr = (d_o/d_i)^3\phi_o Ra \tag{22}$$

where both T_o and ϕ_o are circumferentially uniform.

McAdams specifies the power-law form [equation (20)] only for $Ra_o \geqslant 10^4$, while a table of Nu_o vs Ra_o is provided for $Ra_o = 10^3, 10^2, \ldots$. Using the tabular values, individual power-law expressions were constructed here for the Ra_o ranges 10^3–10^4, 10^2–10^3, ... Morgan's correlation is specified by a sequence of power laws for the respective Ra_o ranges $>10^4$, 10^2–10^4, etc. The Churchill–Chu correlation applies for all Ra_o in the laminar range.

In general, equations (17) and (18), supplemented by one of the Nu_o, Ra_o correlations, are not sufficient for the determination of the heat transfer rate. This is because the temperature ϕ_o [i.e. $(T_o - T_\infty)$] at the outer surface of the insulation is unknown and, therefore, so are Ra_o and Nu_o. To facilitate the determination of ϕ_o and Ra_o, a supplementary equation based on heat transfer continuity is readily derived as

$$\phi_o = 2(k_{ins}/k_{air})/Nu_o R \tag{23}$$

where R is given by equation (18).

For prescribed values of the parameters Ra, k_{ins}/k_{air}, d_o/d_i and Nu_i, the corresponding values of ϕ_o, Nu_o and Ra_o may be found by a simple iterative scheme. With a trial value of ϕ_o, equation (22) yields Ra_o, and the corresponding Nu_o follows from equations (20) or (21). Then, R is evaluated from equation (18) and, with k_{ins}/k_{air}, Nu_o and R, an updated value of ϕ_o is obtained from equation (23). A new cycle of the iteration is then initiated and the process continued until convergence. The procedure is readily automated, and a root-finder technique such as the Newton–Raphson method can be employed to advantage.

With Nu_o thus determined, the heat transfer rate follows from equation (17). The use of the one-dimensional model for the evaluation of the critical radius will be described later.

RESULTS AND DISCUSSION

Heat transfer

Figures 2–5 have been prepared to compare the heat transfer results from the one- and two-dimensional

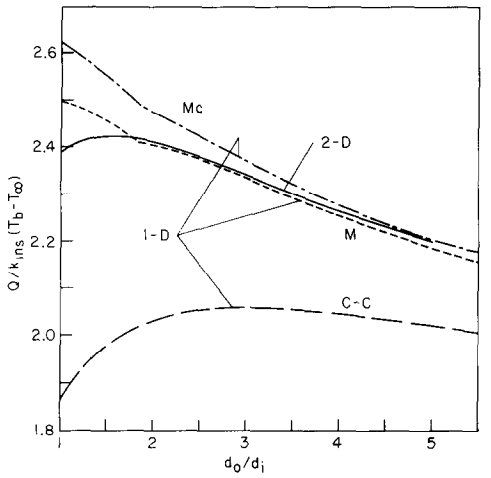

FIG. 2. Heat transfer results from the one- and two-dimensional models, $k_{ins}/k_{air} = 2$, $Ra = 20$, $Nu_i = \infty$.

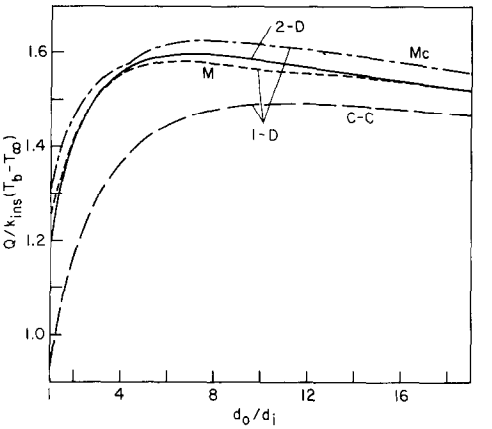

FIG. 4. Heat transfer results from the one- and two-dimensional models, $k_{ins}/k_{air} = 4$, $Ra = 20$, $Nu_i = \infty$.

models and also to assess the sensitivity of the one-dimensional results to the various Nu_o, Ra_o correlations. Each figure corresponds to a horizontal cylinder with a fixed outside diameter d_i and fixed overall temperature difference $(T_b - T_\infty)$ as specified by the value of the Rayleigh number Ra. Insulation whose thermal conductivity relative to air is indicated by the k_{ins}/k_{air} ratio is added parametrically as d_o/d_i increases. The response of the cylinder heat loss to the addition of the insulation is conveyed by the variation of $Q/k_{ins}(T_b - T_\infty)$ with d_o/d_i.

In view of the number of parameters, the results are, necessarily, representative rather than all-inclusive. Figures 2 and 3 are for $k_{ins}/k_{air} = 2$, with $Ra = 20$ and 1000, while Figs. 4 and 5 are for $k_{ins}/k_{air} = 4$ and for the same values of Ra. In all of the figures, $Nu_i = \infty$. In each figure, there are four curves. One (the solid line) represents the present two-dimensional solutions, while the other three represent the one-dimensional results based respectively on the correlations of McAdams, Morgan, and Churchill and Chu (designated as Mc, M, and C–C).

An overall inspection of the figures shows that there can be a substantial correlation-related difference in the heat transfer results yielded by the one-dimensional model. For the cases investigated, the highest and lowest Q values respectively stem from the McAdams and Churchill–Chu correlations, with those from the Morgan correlation falling in between.

It is also seen that for all cases, heat transfer results from the present two-dimensional solutions are bracketed between the highest and lowest predictions from the one-dimensional model. Thus, the overall correlation-related uncertainty in the one-dimensional results is greater than the differences between the one- and two-dimensional heat transfer results. Among the three sets of one-dimensional predictions, those based on the Morgan correlation are consistently closest to the two-dimensional results. On this basis, it is recommended that when one-dimensional heat loss

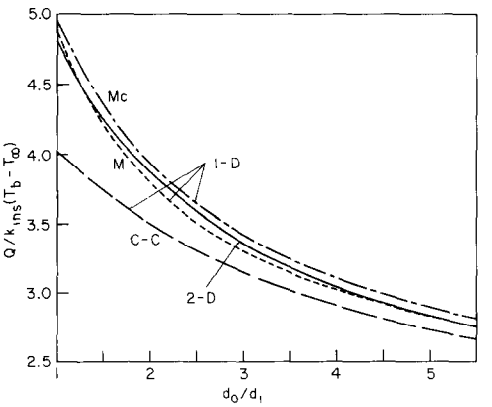

FIG. 3. Heat transfer results from the one- and two-dimensional models, $k_{ins}/k_{air} = 2$, $Ra = 1000$, $Nu_i = \infty$.

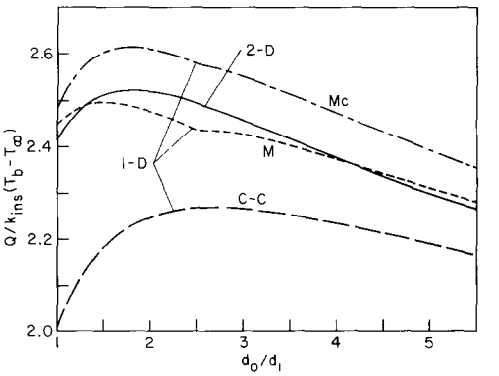

FIG. 5. Heat transfer results from the one- and two-dimensional models, $k_{ins}/k_{air} = 4$, $Ra = 1000$, $Nu_i = \infty$.

calculations are made, the Morgan correlation be used for the natural convection Nusselt number.

Further examination of the figures shows a variety of patterns in the curves of $Q/k_{ins}(T_b - T_\infty)$ vs d_o/d_i. In this regard, it may be noted that if there is a maximum at which the slope of the curve is horizontal, that maximum corresponds to the critical radius of the insulation. In Fig. 2, a critical radius is displayed both by the two-dimensional Q distribution and by the one-dimensional distribution based on the Churchill–Chu correlation, but not by the other two one-dimensional distributions. No critical radii are displayed in Fig. 3 since for the relatively low k_{ins} value implied by $k_{ins}/k_{air} = 2$, the external convective resistance associated with $Ra = 1000$ is too small to trigger the conduction–convection competition needed for the attainment of the critical radius. In Figs. 4 and 5, all of the curves display a critical radius. Note may also be taken of local changes in slope of the McAdams-based and Morgan-based curves. These changes are due to changes in the constants C and n of the power-law representation (20).

It is also relevant to enquire whether the quality of the agreement between the critical radius results of the one- and two-dimensional models foretells anything about the level of agreement of the Q distribution curves. In this regard, attention may be turned to Fig. 5. There, it is seen that the critical radius for the McAdams-based Q distribution is virtually identical to that for the two-dimensional model, while the Morgan-based distribution displays a smaller critical radius. Notwithstanding this, the Morgan distribution is closer to that for the two-dimensional model.

In Fig. 4, the critical radius for the McAdams curve is, again, closer to that for the two-dimensional case than is the Morgan value, but the Morgan-based heat transfer distribution is, also again, a better approximation to the two-dimensional distribution. In all cases, the critical radius for the curve based on the Churchill–Chu correlation is substantially different from the two-dimensional value, and the Churchill–Chu Q distribution is also off the mark. From the foregoing discussion, it appears that the quality of the critical radius prediction is not a definitive tell-tale for the quality of the heat transfer prediction.

Critical radius

The procedures used to determine the critical radius will be described as a prelude to the presentation of the results. Considering first the two-dimensional solutions, it may be noted that graphs such as Figs. 2, 4 and 5, while useful for identifying the general neighborhood of the critical radius, do not provide the degree of resolution needed for high accuracy. To achieve the desired accuracy, the critical radius was obtained from a polynomial fitted to points in the neighborhood of the critical.

For the one-dimensional model, a set of critical radius results was determined by employing the traditional criterion

$$h_o r^*/k_{ins} = 1. \tag{24}$$

In the derivation of equation (24), the dependence of h_o on d_o and on $(T_o - T_\infty)$ is neglected. As a consequence, the critical radius given by equation (24) does not actually correspond to the maximum of curves of $Q/k_{ins}(T_b - T_\infty)$ vs d_o/d_i such as those of Figs. 2, 4 and 5.

To apply equation (24) to the determination of d_o/d_i at the critical radius, it is first relevant to note that $h_o r^*/k_{ins} = 1$ is equivalent to $Nu_o = 2(k_{ins}/k_{air})$ and, with this, the correlations (20) and (21) become

$$2(k_{ins}/k_{air}) = CRa^n(d_o/d_i)^{3n}\phi_o^n \tag{20a}$$

$$2(k_{ins}/k_{air}) = C_1 + C_2 Ra^{1/4}(d_o/d_i)^{3/4}\phi_o^{1/4}. \tag{21a}$$

These equations contain ϕ_o as an unknown in addition to d_o/d_i. An additional relation between d_o/d_i and ϕ_o is obtained by specializing equation (23), which becomes

$$\phi_o = [2(k_{ins}/k_{air})/Nu_i + \ln(d_o/d_i) + 1]^{-1}. \tag{23a}$$

For given values of Ra, k_{ins}/k_{air} and Nu_i, equations (20a)/(21a) and (23a) can be solved to obtain the value of d_o/d_i corresponding to the critical radius. Here again, root-finder techniques may be used advantageously. Notwithstanding this, the task of implementing the $h_o r^*/k_{ins} = 1$ criterion is considerably more complex than is suggested by its simple form.

Another set of critical radius results was obtained which truly reflects the maximum heat transfer rates predicted by the one-dimensional model. These results may be determined from curves of $Q/k_{ins}(T_b - T_\infty)$ vs d_o/d_i or, alternatively and more efficiently, by using the finding of [4] which states that when Nu_o is expressed by a power law such as equation (20), the critical radius criterion is

$$h_o r^*/k_{ins} = 3n/(1+n) \equiv N. \tag{25}$$

To extract the d_o/d_i ratio corresponding to the critical radius, operations involving equations (20), (22), (23) and (25) yield

$$A(d_o/d_i)^3 - \ln(d_o/d_i) - B = 0 \tag{26}$$

in which

$$A = Ra/N[N(2/C)(k_{ins}/k_{air})]^{1/n} \tag{27}$$

$$B = [2(k_{ins}/k_{air})/Nu_i + 1/N]. \tag{28}$$

For given values of Ra, k_{ins}/k_{air} and Nu_i, and for a specified power law (C, n), the constants A and B are known, and equation (26) can be solved for d_o/d_i by a root-finder technique.

The just-described methodology can be extended so as to be applicable when the Nu_o, Ra_o relationship is not a power law, e.g. equation (21). In this case, a trial value of Ra_o which corresponds to the critical radius condition is chosen, and Nusselt numbers corresponding to Ra_o, $0.99Ra_o$, and $1.01Ra_o$ are evaluated from the Nu_o, Ra_o relationship. A power law $Nu_o = CRa_o^n$ is then fitted between the $0.99Ra_o$ and $1.01Ra_o$ points. With C and n, the critical value of d_o/d_i is found from equation (26). Also, with this d_o/d_i and with the value of Nu_o corresponding to the guessed Ra_o, equation (23) is used

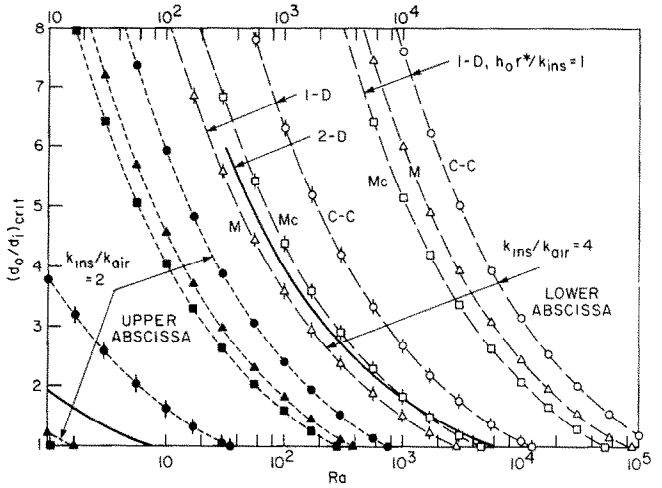

FIG. 6. Critical radius results from the one- and two-dimensional models, $Nu_i = \infty$, $k_{ins}/k_{air} = 2$ and 4.

to determine ϕ_o. Then, from the product $Ra(d_o/d_i)^3\phi_o$, a new value of Ra_o is calculated, and, with it, a new cycle of the iteration is initiated. The procedure is then continued until convergence.

It is noteworthy that use of equation (25) yields values of the critical radius that are identical to those obtained by automated examination of the Q/k_{ins} $(T_b - T_\infty)$ vs d_o/d_i distributions. The perfect agreement was found to occur both when the Nu_o, Ra_o relation is a power law and is not a power law [e.g. equation (21)]. It is also noteworthy that the generalization of equation (25), as described in the preceding paragraph, provides a method much simpler than that of [5] for determining r^* when the Nu_o, Ra_o relation is not a power law.

The numerical results for the critical radius are presented in Figs. 6–9 in terms of the d_o/d_i ratio, i.e. $r^* = \frac{1}{2}(d_o)_{crit}$. Figures 6 and 7 convey the results corresponding to $Nu_i = \infty$, the upper limit of the pipe-flow Nusselt number, while Figs. 8 and 9 are for the lower limit $Nu_i = 4$. The results are also parameterized by k_{ins}/k_{air}, respectively 2 and 4 in Figs. 6 and 8, and 3 and 5 in Figs. 7 and 9.

Each figure has a common format which is labeled in detail in Fig. 6 but to a lesser extent in the other figures to avoid crowding. Turning first to Fig. 6, it is seen that the curves in the right-hand portion of the figure are for $k_{ins}/k_{air} = 4$ and are referred to the Ra values on the lower abscissa, while those in the left-hand portion are for $k_{ins}/k_{air} = 2$ and referred to the Ra on the upper abscissa. For each k_{ins}/k_{air}, there are seven sets of results, as indicated for the $k_{ins}/k_{air} = 4$ case.

The rightmost cluster of three dashed curves is for the one-dimensional model with the traditional $h_o r^*/k_{ins} = 1$ criterion, while the next-to-rightmost cluster of three dashed curves represents the true critical radius results for the one-dimensional model. These curves are

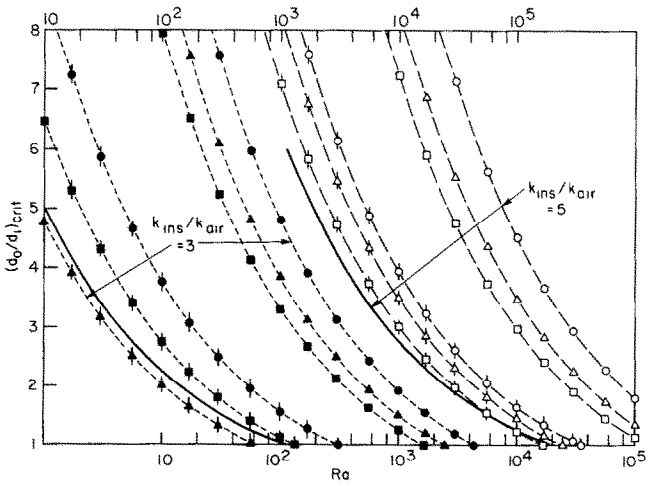

FIG. 7. Critical radius results from the one- and two-dimensional models, $Nu_i = \infty$, $k_{ins}/k_{air} = 3$ and 5.

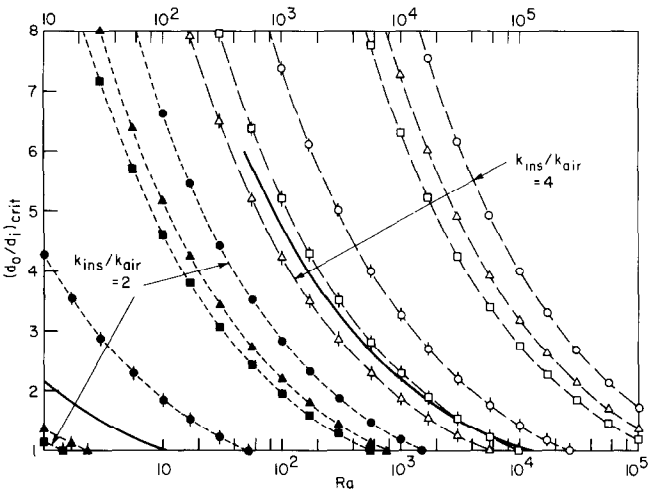

FIG. 8. Critical radius results from the one- and two-dimensional models, $Nu_i = 4$, $k_{ins}/k_{air} = 2$ and 4.

identified by the letters M, Mc, and C–C, respectively denoting the Morgan, McAdams, and Churchill–Chu correlations on which the individual curves are based. Note that the data symbols which periodically punctuate each curve are intended to serve as identifiers—a triangle for Morgan, a square for McAdams, and a circle for Churchill and Chu. Unflagged and flagged symbols are used to distinguish between the one-dimensional cases with and without the $h_o r^*/k_{ins} = 1$ constraint. The heavy black line labeled 2-D represents the critical radius results from the present two-dimensional solutions.

A similar pattern of identification applies to the $k_{ins}/k_{air} = 2$ curves in Fig. 6, but the labels have been omitted because of the lack of space. Note also that the identifying symbols have been blackened to make a clear distinction between the two k_{ins}/k_{air} values. In Figs. 7–9, only the k_{ins}/k_{air} tie lines are indicated, but the remainder of the labeling from Fig. 6 carries over intact.

Each curve in Figs. 6–9 represents the variation of the critical radius, expressed in terms of $(d_o/d_i)_{crit}$, with the Rayleigh number Ra which is based on d_i and $(T_b - T_\infty)$. For all cases, the critical radius decreases as Ra increases. This trend reflects the lower convective resistance associated with larger Ra and the lesser thickness of insulation at which the increase in the conductive resistance with d_o overcomes the decrease in the convective resistance.

Another major finding which strongly manifests itself in all the figures is the significant deviation between the one-dimensional results based on $h_o r^*/k_{ins} = 1$ and the results of both the true one-dimensional model and the two-dimensional model. In all cases, the $h_o r^*/k_{ins} = 1$ condition yields values of the critical radius that are too high. These overly large values of r^* discourage the use of insulation (or of additional

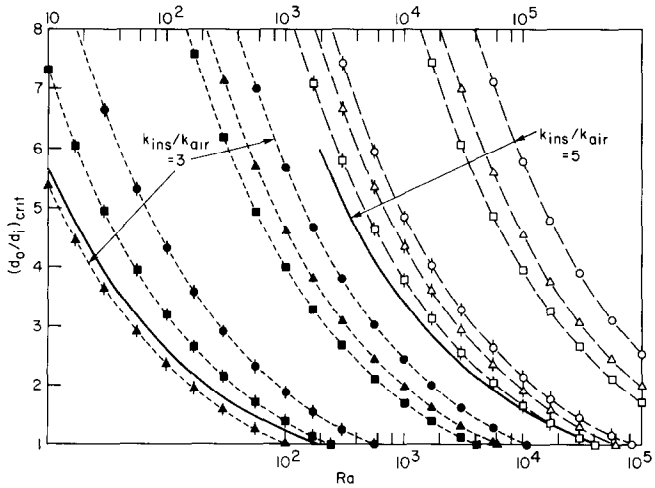

FIG. 9. Critical radius results from the one- and two-dimensional models, $Nu_i = 4$, $k_{ins}/k_{air} = 3$ and 5.

insulation) when, in fact, the insulation would be advantageous. The critical radii based on $h_o r^*/k_{ins} = 1$ are so far off the mark that the continued use of the $h_o r^*/k_{ins} = 1$ condition is a disservice. It is recommended that this condition no longer be included in textbooks on heat transfer.

Further inspection of the figures reveals that the critical-radius predictions from the one-dimensional model depend substantially on the Nu_o correlation used in the numerical evaluation of the model. In particular, for the true one-dimensional model (i.e. without the $h_o r^*/k_{ins} = 1$ condition), the correlation-related spread of the predictions brackets the two-dimensional results (heavy black line) in six of the eight cases contained in Figs. 6–9. The bracketing occurs for all $k_{ins}/k_{air} \leqslant 4$. Therefore, for this range, which represents the range of quality insulating materials, the correlation-related uncertainties in the one-dimensional results exceed the differences between the one- and two-dimensional results.

It is also seen that among the three one-dimensional predictions for the critical radius, that based on the Churchill–Chu correlation is the highest and is the most deviant from the two-dimensional results. For $k_{ins}/k_{air} = 5$, the McAdams-based predictions are the closest of the one-dimensional results to those of the two-dimensional model, while for $k_{ins}/k_{air} = 4$, the McAdams-based predictions are slightly better than the Morgan-based predictions. For $k_{ins}/k_{air} = 3$ and 2, the Morgan-based predictions are better. Therefore, if the one-dimensional model is to be used for predicting the critical radius, Nu_o should be evaluated from the McAdams correlation for $k_{ins}/k_{air} > 4$ and from the Morgan correlation for $k_{ins}/k_{air} < 4$.

Although Figs. 6–9 convey highly useful comparisons between the various models, the effects of the k_{ins}/k_{air} and Nu_i parameters on the critical radius are not definitively portrayed. This is accomplished in Fig. 10, which displays the two-dimensional results for the critical radius. The figure shows that the critical radius is a strong function of k_{ins}/k_{air}, increasing as k_{ins}/k_{air}

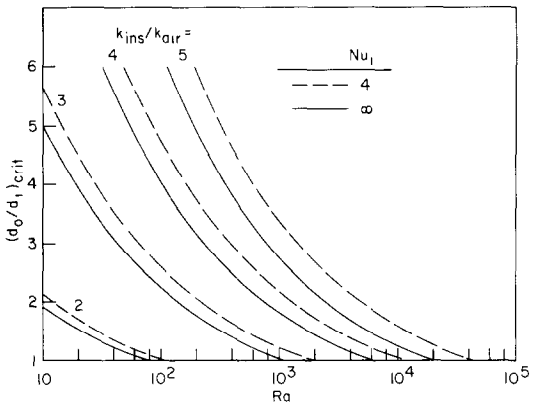

FIG. 10. Parametric dependences of the critical radius results from the two-dimensional model.

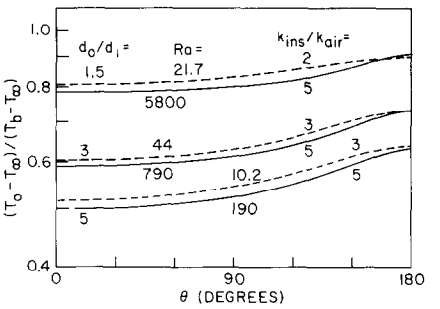

FIG. 11. Representative circumferential temperature distributions on the outer surface of the insulation.

increases. The increase reflects the tendency toward diminished conductive resistance at larger k_{ins}/k_{air} and the greater thickness of insulation that counteracts this tendency. On the other hand, the critical radius depends only weakly on the pipe-flow Nusselt number Nu_i, whose assigned range of 4–∞ spans the entire range of practically attainable values. The insentitivity to Nu_i can be traced to the fact that the internal convective resistance is only a small part of the overall thermal resistance.

Circumferential temperature variations

Representative results for the circumferential variation of the temperature T_o on the outer surface of the insulation are presented in Fig. 11. The cases for which results are displayed were selected by first choosing d_o/d_i [the dominant parameter for the $T_o(\theta)$ variation] and then taking the k_{ins}/k_{air} and Ra parameters from Figs. 6 and 7, which correspond to $Nu_i = \infty$.

From Fig. 11, it is seen that for each circumferential distribution, the minimum temperature occurs at the lower stagnation point $\theta = 0°$. The temperature increases monotonically with θ and attains a maximum at the upper stagnation point $\theta = 180°$, with most of the increase occurring in the upper half of the cylinder, i.e. for $\theta > 90°$. This variation in T_o reflects the circumferential distribution of the convective heat transfer coefficient, which takes on its largest value at $\theta = 0°$ and decreases monotonically as θ increases. The largest overall increase of the dimensionless temperature between the lower and upper stagnation points is about 25%.

The figure also shows that, as expected, the thicker the insulation layer, the lower is the temperature at the outer surface of the insulation. Conclusions should not be drawn from the figure about the effect of k_{ins}/k_{air} on the temperature distribution because the two k_{ins}/k_{air} curves for each d_o/d_i do not correspond to the same value of Ra.

CONCLUDING REMARKS

This paper has been concerned not only with the conjugate, two-dimensional conduction–convection

problem for heat transfer from an insulated horizontal cylinder to air, but also with an in-depth examination of one-dimensional radial heat flow models of the problem. For the numerical evaluation of the one-dimensional model, the required values of the circumferential-average natural convection heat transfer coefficient at the outer surface of the insulation were taken from the three most commonly used correlations—McAdams, Morgan, and Churchill and Chu.

It was found that there can be a substantial correlation-related difference in the heat transfer results yielded by the one-dimensional model. The overall correlation-related uncertainty in the one-dimensional results is greater than the differences between the one- and two-dimensional heat transfer results. Among the competing correlations, that of Morgan yields one-dimensional results which agree most closely with those from the two-dimensional conjugate solutions. On this basis, it is recommended that when one-dimensional heat loss calculations are made, the Morgan correlation be used for the natural convection heat transfer coefficient.

Results for the critical radius were also obtained. For the one-dimensional model, the critical radius was evaluated both for the conventional $h_o r^*/k_{ins} = 1$ condition and for the true maximum heat transfer condition. The $h_o r^*/k_{ins} = 1$ condition is approximate in that it neglects the dependence of the natural convection heat transfer coefficient on both the outer radius of the insulation and the surface-to-ambient temperature difference. The critical radius for the two-dimensional model corresponds to the maximum rate of heat transfer.

The critical radius results corresponding to the $h_o r^*/k_{ins} = 1$ condition were found to be substantially in error and always on the high side. It is recommended that this condition no longer be included in textbooks on heat transfer.

For $k_{ins}/k_{air} \leqslant 4$, the correlation-related uncertainties in the critical radius predictions from the true one-dimensional model exceed the differences between the one- and two-dimensional results. On the basis of comparisons with the two-dimensional results, it is recommended that when the one-dimensional model is used for predicting the critical radius, the natural convection Nusselt number should be evaluated from the McAdams correlation for $k_{ins}/k_{air} > 4$ and from the Morgan correlation for $k_{ins}/k_{air} < 4$.

It was demonstrated that the most efficient method of calculating the true critical radius for the one-dimensional model is the condition $h_o r^*/k_{ins} = 3n/(1+n)$, where n is the exponent of a Nusselt–Rayleigh power law. An efficient procedure was developed for using this condition even when the Nusselt–Rayleigh relation is not a power law.

The critical radius was found to be sensitive both to the Rayleigh number (based on the outer diameter of the pipe and the overall temperature difference) and the conductivity ratio k_{ins}/k_{air}, but was insensitive to the Nusselt number of the flow inside the pipe.

REFERENCES

1. W. H. McAdams, *Heat Transmission* (3rd edn). McGraw-Hill, New York (1954).
2. V. T. Morgan, The overall convective heat transfer from smooth circular cylinders. In *Advances in Heat Transfer* (Edited by T. F. Irvine, Jr and J. P. Hartnett), Vol. 11. Academic Press, New York (1975).
3. S. W. Churchill and H. H. S. Chu, Correlating equations for laminar and turbulent free convection from a horizontal cylinder, *Int. J. Heat Mass Transfer* **18**, 1049–1053 (1975).
4. E. M. Sparrow, Reexamination and correction of the critical radius for radial heat conduction, *A.I.Ch.E. Jl* **16**, 149 (1970).
5. R. T. Balmer, The critical radius effect with a variable heat transfer coefficient, *A.I.Ch.E. Jl* **24**, 547–548 (1978).
6. L. D. Simmons, Critical thickness of insulation accounting for variable convection coefficient and radiation loss, *J. Heat Transfer* **98**, 150–152 (1976).
7. T. H. Kuehn, Radial heat transfer and critical Biot number with radiation, uniform surface heat generation, and curvature effects in convection, *J. Heat Transfer* **100**, 374–376 (1978).
8. T. H. Kuehn and R. J. Goldstein, Numerical solution to the Navier–Stokes equations for laminar natural convection about a horizontal isothermal circular cylinder, *Int. J. Heat Mass Transfer* **23**, 971–979 (1980).

TRANSFERT THERMIQUE BIDIMENSIONNEL ET RAYON CRITIQUE POUR LA CONVECTION NATURELLE AUTOUR D'UN CYLINDRE HORIZONTAL CALORIFUGE

Résumé—Le problème du transfert thermique bidimensionnel (radial et circonférentiel) et de l'écoulement du fluide pour un cylindre horizontal calorifugé qui perd de la chaleur par convection naturelle d'air est analysé en résolvant la forme différentielle des lois de conservation. Il en résulte un problème conjugué de conduction dans la couche isolante et de convection naturelle dans l'air ambiant. Un problème monodimensionnel de flux radial est aussi étudié en détail; les coefficients de convection moyen suivant la circonférence qui sont nécessaires sont pris respectivement à partir des formules de MacAdams, Morgan et Churchill et Chu. On trouve que la dispersion, dues à ces formules, des résultats de transfert à partir du modèle monodimensionnel est plus grande que les différences entre les résultats mono et bidimensionnels. L'utilisation de la formule de Morgan donne les résultats de transfert monodimensionnel les plus précis. Pour le rayon critique, le critère classique $h_0 r^*/k_{inst} = 1$ conduit à des erreurs sensibles et ne peut pas toujours être utilisé. Les résultats de rayon critique à partir du modèle monodimensionnel peuvent être calculés efficacement à partir du critère $h_0 r^*/k_{inst} = 3n/(1+n)$, où n'est un paramètre déterminé pour chaque formulation spécifique Nusselt–Rayleigh.

ZWEIDIMENSIONALE WÄRMEÜBERTRAGUNG UND ERGEBNISSE FÜR DEN KRITISCHEN RADIUS BEI NATÜRLICHER KONVEKTION AN EINEM ISOLIERTEN HORIZONTALEN ROHR

Zusammenfassung—Das zweidimensionale (radiale und tangentiale) Wärmeübertragungs- und Strömungsproblem bei einem flüssigkeitsdurchströmten, isolierten horizontalen Rohr, das durch natürliche Konvektion Wärme an Luft abgibt, wurde durch Lösen der Differentialform des Erhaltungsgesetzes analysiert. Das sich ergebende zugeordnete Problem beinhaltet Wärmeleitung in der Isolierschicht und natürliche Konvektion an die umgebende Luft. Ein eindimensionales, radiales Wärme-Strömungs-Modell für das Problem wurde außerdem im Detail untersucht, und die für die Berechnung benötigten über den Umfang gemittelten Wärmeübergangskoeffizienten bei natürlicher Konvektion wurden den allgemein gebräuchlichen Beziehungen von McAdams, Morgan, sowie Churchill und Chu entnommen. Es wurde herausgefunden, daß der beziehungsabhängige Streubereich der Wärmeübertragungsergebnisse des eindimensionalen Modells größer war als die Unterschiede zwischen eindimensional und zweidimensional berechneten Ergebnissen. Die Verwendung der Morgan-Ergebnisse ergab die genauesten eindimensional berechneten Wärmeübertragungsergebnisse, (d.h. die beste Übereinstimmung mit den zweidimensional berechneten Ergebnissen). Für den kritischen Radius führte das Standard-Kriterium $h_0 r^*/k_{ins} = 1$ zu wesentlichen Fehlern und sollte nicht weiter verwendet werden. Die Ergebnisse zum kritischen Radius nach dem eindimensionalen Modell, obgleich beziehungsabhängig und abweichend von den zweidimensional berechneten Ergebnissen, können wirkungsvoll und genau mit dem Kriterium $h_0 r^*/k_{ins} = 3n/(1+n)$ berechnet werden, wobei n ein Exponent ist, der für jede Nusselt–Rayleigh-Beziehung bestimmt werden kann.

РЕЗУЛЬТАТЫ ПО ДВУМЕРНОМУ ТЕПЛОПЕРЕНОСУ И КРИТИЧЕСКОМУ РАДИУСУ ДЛЯ ЕСТЕСТВЕННОЙ КОНВЕКЦИИ ВОКРУГ ИЗОЛИРОВАННОГО ГОРИЗОНТАЛЬНОГО ЦИЛИНДРА

Аннотация—Путем решения дифференциальных уравнений, выражающих законы сохранения, проанализирован двумерный (в координатах: радиус, полярный угол) теплообмен и течение жидкости в изолированном горизонтальном цилиндре, теплообмен которого с воздухом осуществляется естественной конвекцией. Полученная в результате сопряженная задача описывает теплопроводность в слое изоляции и естественную конвекцию в окружающем воздухе. Детально изучалась также модель одномерного, радиального теплового потока, а средние коэффициенты теплопередачи при естественной конвекции вокруг цилиндра, необходимые для ее оценки, были, соответственно, взяты из известных соотношений МакАдамса, Моргана, Черчилля и Чу. Найдено, что расхождение результатов по теплообмену, полученных с использованием разных соотношений одномерной модели, больше, чем различия между результатами по одно-и двумерной моделям. Применение соотношения Моргана дало самые точные данные по одномерному теплообмену (т.е. наблюдалось наилучшее совпадение с результатами двумерной модели). Для критического радиуса стандартный критерий $h_0 r^*/k_{ins} = 1$ приводил к существенным ошибкам и не рекомендован к дальнейшему использованию. Результаты по критическому радиусу из одномерной модели хотя и зависят от используемых соотношений и имеют расхождение с двумерными результатами, однако могут быть эффективно и точно рассчитаны при помощи критерия $h_0 r^*/k_{ins} = 3n/(1+n)$, где n—экспонента, которую можно определить для каждой конкретной зависимости Нуссельта от Рэлея.